

NMR Determination of Amide N-H Equilibrium Bond Length from Concerted Dipolar Coupling Measurements

Lishan Yao, Beat Vögeli, Jinfa Ying, and Ad Bax

Laboratory of Chemical Physics, NIDDK, National Institutes of Health, Bethesda, MD 20892-0520

Theoretical Analysis

RDCs measured in multiple alignments can be expressed as:^{1,2}

$$\mathbf{D}_M = D_{\max}^{IS} \langle \mathbf{B} \rangle \langle \mathbf{A} \rangle \quad (1)$$

where \mathbf{D}_M is the $L \times N$ RDC matrix and \mathbf{B} is an $L \times 5$ matrix, each row of which is a vector b :

$$b = \left\{ (3z^2 - 1)/2, \frac{\sqrt{3}}{2}(x^2 - y^2), \sqrt{3}xz, \sqrt{3}yz, \sqrt{3}xy \right\}, \quad (2)$$

where (x, y, z) are the Cartesian coordinates of the internuclear vector. \mathbf{A} is a $5 \times N$ matrix, each column of which is a vector a . The vector a has the same form as b , but with x, y, z denoting the orientation of the magnetic field in the molecular frame. D_{\max}^{IS} is a constant, defined as

$$D_{\max}^{IS} = -\mu_0 \hbar \gamma_I \gamma_S \langle r_{IS}^{-3} \rangle / 4\pi^2 \quad (3)$$

where μ_0 is the magnetic permittivity of vacuum, \hbar is the Planck's constant, γ_X is the gyromagnetic ratio of spin X, and r_{IS} is the inter-nuclear distance. By assuming a group of residues with only symmetric motions of uniform amplitude, described by an order parameter S , eq 1 can be written as

$$\mathbf{D}_M = \mathbf{B} \mathbf{A} \mathbf{m} \quad (4)$$

with the apparent alignment matrix $\mathbf{A} \mathbf{m}$ given by:

$$\mathbf{A} \mathbf{m} = -\mu_0 \hbar \gamma_I \gamma_S \langle r_{IS}^{-3} \rangle S \langle \mathbf{A} \rangle / 4\pi^2 \quad (5)$$

If two types of RDCs are measured in a given macromolecule, such as C^α -C' and N-H^N in the present study, the apparent alignment matrix element ratio is

$$\frac{\mathbf{A} \mathbf{m}(C' C \alpha)}{\mathbf{A} \mathbf{m}(NH)} = \frac{\gamma_C \gamma_C S_{C' C \alpha} \left\langle \frac{1}{r_{C' C \alpha}^3} \right\rangle}{\gamma_N \gamma_H S_{NH} \left\langle \frac{1}{r_{NH}^3} \right\rangle} \quad (6)$$

The apparent alignment matrix of N-H is determined by using the iterative DIDC method,² starting from the GB3 NMR-refined X-ray structure (PDB entry 2OED). Use of the 2OED starting structure results in 100% convergence, but the results do not depend on the starting point.² A total of 45 residues are included in the procedure, with the remaining 11 being filtered out because of fast amide proton exchange with solvent (N-terminal 2 residues), by resonance overlap in one or more of the mutants (5 residues), or due to elevated dynamics, as identified by the iterative DIDC protocol² (4 residues). The

same iterative DIDC procedure is used to determine the alignment matrices of the C^α-C' bond vectors for the five mutants.

This study evaluated the dynamics of the N-H bond relative to a frame defined by the C^α-C' bond vectors. Isotropic internal motions of rigid peptide groups to a first approximation impacts N-H and C^α-C' bond vectors equally and factors out in our dynamics evaluation. The N-H bond dynamics relative to the C/N-atom frame remains, however, as does the effect of anisotropy of the peptide plane motion about the C^α-C^α axis (so-called γ motions).^{3,4} Here we build a coordinate system, with the origin on the amide N atom, the z axis parallel to the time-averaged N-H orientation, the y axis in the plane defined by C', N and H^N, and the x axis perpendicular to this plane. The displacement distribution function of H^N in this frame is defined as $\rho(r, \theta, \phi)$, where (r, θ, ϕ) are the H^N polar coordinates. To a good approximation, the bond stretching motion and angular libration are separable, so that

$$\rho(r, \theta, \phi) \approx \rho_1(r)\rho_2(\theta, \phi) \quad (7)$$

Below, we will treat bond stretching using quantum statistical mechanics, but approximate angular fluctuations by Gaussian distributions, in agreement with classical statistical mechanics when the amplitude of the librations is small.

N-H bond stretching

The stretching motion around the equilibrium bond length can be described by harmonic oscillation with a small anharmonic correction. The approximate energy potential is:

$$E = E_0 + \frac{1}{2}k(r - r_{eq})^2 + \frac{1}{6}f(r - r_{eq})^3 \quad (8)$$

where r_{eq} is the equilibrium bond length, E_0 is the energy in the equilibrium, k and f are force constants. E_0 acts as a reference and has no influence on the distribution function, and is therefore omitted in the derivation below. Instead of solving the Schrödinger equation for the energy function of eq 8, we first solve the equation for an ideal quantum harmonic oscillator and subsequently use first order perturbation theory to include the effect of anharmonicity. For a quantum oscillator with the Hamiltonian

$$H = \frac{p^2}{2m} + \frac{1}{2}m\omega^2 x^2 \quad (9)$$

where $\omega = (k/m)^{1/2}$, the solution of the Schrödinger equation is,⁵

$$\psi_n(x) = \sqrt{\frac{1}{2^n n!}} \left(\frac{m\omega}{\pi\hbar} \right)^{1/4} \exp\left(-\frac{m\omega x^2}{2\hbar}\right) H_n\left(\sqrt{\frac{m\omega}{\hbar}} x\right) \quad (10)$$

in which

$$H_n(x) = (-1)^n \exp(x^2) \frac{d^n}{dx^n} \exp(-x^2) \quad (11)$$

$$E_n = \hbar\omega(n + 1/2) \quad (12)$$

The equilibrium wave function in the canonical ensemble then is given by

$$\psi_{eq}(x) = \frac{\sum \exp(-E_n / k_B T) \psi_n(x)}{\sum \exp(-E_n / k_B T)} \quad (13)$$

where k_B is the Boltzmann constant and T is the temperature. It is worth noting that the energy difference between the ground state ($n=0$) and the first excited state ($n=1$) equals ~ 10 kcal/mol for the N-H stretching motion, where $k_B T$ is ~ 0.6 kcal/mol in room temperature. The coefficient of the first excitation state in eq 13 is $\sim 10^7$ times smaller than for the ground state, and all excited states may be safely ignored, simplifying eq 13 to:

$$\psi_{eq}(x) \approx \psi_0(x) = \left(\frac{m\omega}{\pi\hbar}\right)^{1/4} \exp\left(-\frac{m\omega x^2}{2\hbar}\right) \quad (14)$$

The fluctuation of x is

$$\langle x^2 \rangle = \int_{-\infty}^{+\infty} x^2 \psi_0^*(x) \psi_0(x) dx = \frac{\hbar}{2m\omega} \quad (15)$$

equal to what was obtained by quantum statistics,⁶ in the limit $\hbar\omega \gg k_B T$:

$$\langle x^2 \rangle = \frac{\hbar}{2m\omega} \coth \frac{\hbar\omega}{2k_B T} . \quad (16)$$

To consider the effect of anharmonicity on the wave function, first order perturbation theory yields:

$$E = E_0 + H'_{00} + \sum_{m \neq 0} \frac{|H'_{0m}|^2}{E_0 - E_m} + \dots \quad (17)$$

$$\Psi(x) = \psi_0(x) + \sum_{m \neq 0} \frac{H'_{0m}}{E_0 - E_m} \psi_m(x) + \dots \quad (18)$$

where

$$H'_{0m} = \int_{-\infty}^{+\infty} \frac{1}{6} f x^3 \psi_0^*(x) \psi_m(x) dx \quad (19)$$

H'_{0m} can be derived from eqs 10, 11 and 19. Since $\psi_m(x)$ is an odd function when $m=1,3,5,\dots$, and an even function when $m=0,2,4,\dots$, H'_{0m} is zero when m is an even number. For the first odd component one finds:

$$H'_{01} = (4\sqrt{2})^{-1} f \left(\frac{\hbar}{m\omega}\right)^{3/2} \quad (20)$$

where f is the force constant of eq 8. By ignoring the higher order perturbation, the wave function of eq 18 can be approximated by:

$$\Psi(x) = \psi_0(x) - (4\sqrt{2})^{-1} f \hbar^{1/2} m^{3/2} \omega^{5/2} \psi_1(x) \quad (21)$$

It is then straightforward to calculate $\langle x \rangle$:

$$\langle x \rangle = \frac{\int_{-\infty}^{+\infty} x \Psi^*(x) \Psi(x) dx}{\int_{-\infty}^{+\infty} \Psi^*(x) \Psi(x) dx} = -\frac{f\hbar}{4m^2\omega^3(1+c^2)} \approx -\frac{f}{2m\omega^2} \langle x^2 \rangle \quad (22)$$

where $c = (4\sqrt{2})^{-1} f\hbar^{1/2} m^{3/2} \omega^{5/2}$ and c^2 is very small (see below), permitting the approximation of eq 22, commonly found in the literature.⁷ The non-zero average of $\langle x \rangle$ is caused by anharmonicity of the oscillation. We can then write the density function as

$$\rho_1(x) = \left(\frac{m\omega}{\pi\hbar} \right)^{1/2} \exp\left(-\frac{m\omega x^2}{\hbar} \right) \left(1 - c\sqrt{\frac{2m\omega}{\hbar}} x \right)^2 / (1 + c^2). \quad (23)$$

During the derivation of eq 23, the equilibrium value of x is assumed to be zero. The general form of ρ_1 therefore should be written as:

$$\rho_1(r) = \left(\frac{m\omega}{\pi\hbar} \right)^{1/2} \exp\left(-\frac{m\omega(r - r_{eq})^2}{\hbar} \right) \left(1 - c\sqrt{\frac{2m\omega}{\hbar}}(r - r_{eq}) \right)^2 / (1 + c^2) \quad (24)$$

in which r_{eq} is the equilibrium distance. In our polar coordinate system $r > 0$, whereas the range of x is $[-\infty, +\infty]$ in eq 23. However, the high frequency of the N-H bond stretching restrains r to a very narrow distribution, making it appropriate to use eq 24 for $\rho_1(r)$. To proceed further, we employ the force constants k (1109.8 kcal/mol-Å²) and f (-6577.2 kcal/mol-Å³) calculated for N-methylacetamide N-H bond stretching by MP2 quantum methods⁸ to derive the distribution function $\rho_1(r)$,

$$\rho_1(r) = 5.676 \exp(-103.64(r - r_{eq})^2) (1 + 1.572(r - r_{eq}))^2 \quad (25)$$

The corresponding coefficient c^2 is rather small, only 0.012. From eq 25 one obtains

$$\langle r \rangle = 0.0154 + r_{eq} \quad (26)$$

Another important average is the value of $\langle r^{-3} \rangle^{-1/3}$, which is the pertinent bond length average in RDC and ¹⁵N relaxation studies, denoted r_{eff} in the main text, and can also be evaluated from eq 25. Numeric solution of $r_{eff} - r_{eq}$ and $\langle r \rangle - r_{eq}$ versus r_{eq} are plotted in Figure S2, and show the nearly constant difference between $\langle r \rangle$ and r_{eq} , whereas $r_{eff} - r_{eq}$ scales with r_{eq} .

N-H libration

The next step is to find a suitable angular distribution for the N-H bond libration, describing motions of the proton in directions orthogonal to the time-averaged N-H vector. The librational motion in (θ, ϕ) space is difficult to depict physically, and is more conveniently described by 2D Cartesian coordinates (u, v) of a unit vector with average orientation along z , where u is along x and v along y . Here we assume a 2D Gaussian distributed motion with

$$\rho(u, v) = \frac{1}{2\pi\sigma_u\sigma_v} \exp(-u^2 / 2\sigma_u^2) \exp(-v^2 / 2\sigma_v^2) \quad (27)$$

Together with distribution function $\rho_1(r)$ from eq 25, we have

$$\begin{aligned} \rho(r, u, v) &= \rho(u, v)\rho_1(r) \\ &= \frac{5.676}{2\pi\sigma_u\sigma_v} \exp(-103.64(r - r_{eq})^2) (1 + 1.572(r - r_{eq}))^2 \exp(-u^2 / 2\sigma_u^2) \exp(-v^2 / 2\sigma_v^2) \end{aligned} \quad (28)$$

For $\sigma_{u,v} \ll 1$, the order parameter S and asymmetric motion parameter η then are obtained from:

$$S = (3(1 - \sigma_u^2 - \sigma_v^2) - 1) / 2 \quad (29)$$

$$\eta = (\sigma_v^2 - \sigma_u^2) / S \quad (30)$$

Eq 28 is used as the distribution function for the H atom in the RDC fitting procedure.

Fitting of C'-H^N RDCs

In a first step, the C'-H^N RDCs of 45 rigid residues were fitted to obtain the equilibrium bond length r_{eq} and S with the constraint $\sigma_u^2 = \sigma_v^2$, and using the constraint $S'_{NH} \langle 1/r_{NH}^3 \rangle = 0.872$ obtained from the iterative DIDC analysis. Using the iterative DIDC method and eq 5, the alignment matrix itself is determined from the amide N-H RDCs, which carry the highest measurement precision. The average orientation of each N-H vector is determined from N-H RDCs in separate measurements (see discussion below). The fitting results were shown in table 1 of the main text, with which the explicit form of eq. 28 was obtained,

$$\rho(r, u, v) = \frac{5.676}{0.06\pi} \exp(-103.64(r - 1.008)^2) (1 + 1.572(r - 1.008))^2 \exp(-u^2 / 0.06) \exp(-v^2 / 0.06)$$

In the second step, N-H and C'-H^N RDCs of each secondary structure fragments are fitted without the constraint $\sigma_u^2 = \sigma_v^2$, and allowing for residue-specific S and η values, but with the r_{eq} obtained from the first step. In this two-step fitting process, a numeric distribution of $\rho(r, u, v)$ is generated and used for further analysis.

Besides the acquired N-H RDCs described in the main text, a slightly different series of HNCO experiments were also performed to simultaneously extract ¹⁵N-¹H, ¹³C^α-¹³C' RDCs, without C^α decoupling during C' evolution and ¹H decoupling off during nitrogen evolution. The primary purpose of these experiments was to determine RDCs and residual chemical shift anisotropy contributions to the chemical shifts, which permit extracting CSA of H^N, N and C',¹⁰ which will be discussed in a separate paper. In addition to the five mutants described in the main text, the sixth mutant K19EK4A was also included in these measurements. The six alignments again were determined from N-H RDCs using iterative DIDC, and the average orientation of each N-H vector is calculated by

$$\langle \mathbf{B} \rangle = \frac{1}{D_{\max}^{IS}} \mathbf{D}_M \langle \mathbf{A} \rangle^+ \quad (31)$$

and used for the N-H and C'-H^N RDCs fitting described above. Using H-N-C^α-H^α angles derived from these N-H vector orientations and the C^α-H^α bond vector orientations obtained in our previous study,² fitting of ³J_{HNH^α} values to the Karplus equation gives a record low rmsd of 0.33 Hz (Figure S3).¹¹

The order parameter of each N-H vector can also be obtained from eq 31. But as discussed previously,² the order parameter is far more sensitive to experimental error than the structure. We carried out a two-step procedure to fit experimental RDCs as discussed

in our early study. Initially, the RDCs were fitted using the symmetric motion model, but if the fitting error exceeds the measurement error the fit was repeated using the full five-parameter asymmetric motion model, yielding both S and η values. The resulting S values are plotted in Figure S4. The purpose of the site-specific fitting is to repeat the analysis carried out in our early iterative DIDC paper but with better quality RDCs. The order parameters were compared to relaxation order parameters as well as order parameter from GAF model determined by Blackledge et. al as shown in Fig. S4.

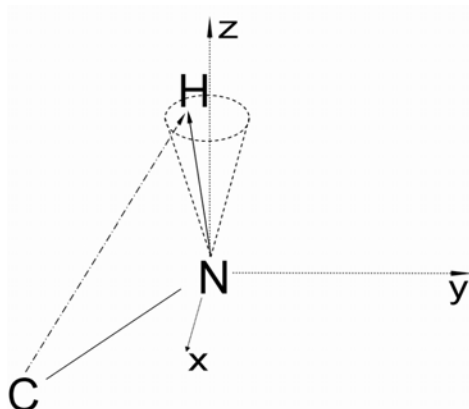


Figure S1. Definition of the coordinate system used (see text). The origin is set at the N atom; C , N and the time-averaged H position fall in the yz plane, and the z axis corresponds to the time-averaged N - H orientation.

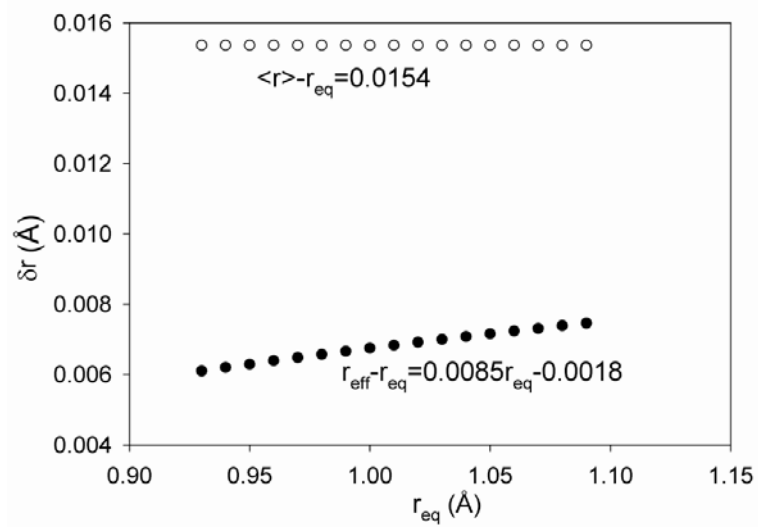


Figure S2. (A) The N-H bond elongation of $\langle r \rangle$ and r_{eff} , where $r_{eff} = 1/\langle r^{-3} \rangle^{1/3}$.

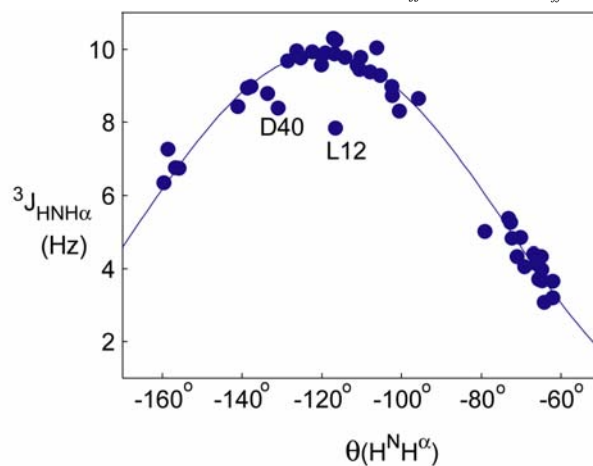


Figure S3. Fit of experimental $^3J_{HNH\alpha}$ values in GB3¹¹ to an optimized Karplus equation, using dihedral angles corresponding to the N-H orientations newly obtained from RDCs (C^α - H^α orientations from Yao et al.²). The rmsd is 0.33 Hz, with mobile residues D40 and L12 not included in the fit and rmsd calculation.

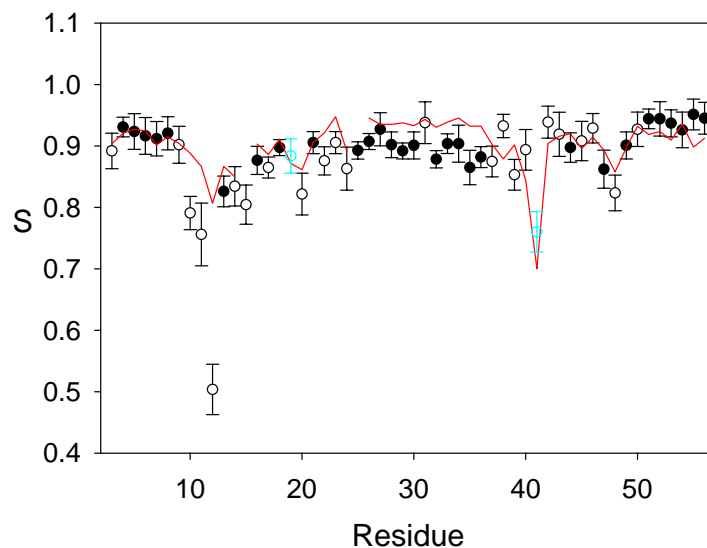


Figure S4. Generalized order parameter, S , of N-H vectors. The filled symbols represent residues that could be fitted to within the experimental RDC error (± 0.3 Hz) with the symmetric motion model, while the open symbols are for residues that required the asymmetric motion model to achieve a satisfactory fit to the RDCs. Residues K19 and G41 (cyan) show small discrepancies of structure or/and dynamics in different mutants, but for completeness are nevertheless included in the figure (in cyan). The red line corresponds to ^{15}N relaxation order parameters derived by Hall and Fushman,¹² using the axially symmetric diffusion model. The relaxation order parameters were scaled by 0.985 to match the bond length 1.015 obtained in this study (vs 1.02 Å used by Hall and Fushman). The RDCs order parameters are scaled by $S_{NH} = S'_{NH} S_{C'C\alpha} = 0.910 \times 0.990 = 0.901$, where 0.990 accounts for the calculated zero-point libration of the $\text{C}'\text{C}^\alpha$ bond vectors ($S_{C'C\alpha} = 0.990$).

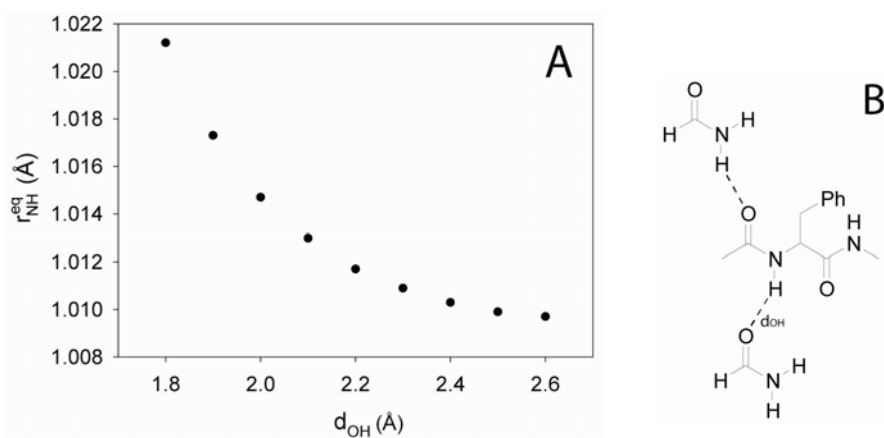


Figure S5. Impact of hydrogen bond length on the N-H equilibrium bond length from DFT calculations for the model system shown in (B). The initial geometry of the system was obtained from the GB3 2OED structure, with the center phenylalanine geometry

taken from F52 and two formamide positions matched to the backbone atoms of its H-bond partners, K4 and D46. The system was geometry optimized at the B3LYP/6-311++G** level using the Gaussian03 program¹³ by restraining all heavy atom dihedral angles of the center residue as well as the positions of the two formamide moieties relative to the peptide backbone, while allowing bond lengths and angles to vary. Then the O-H distance (d_{OH}) was altered stepwise from 1.8Å to 2.6Å by translating the H-bond-accepting formamide along the H...O direction away from the phenylalanine (panel B), after which the entire model system is re-optimized. During this re-optimization, all non-H-atom dihedral angles of the peptide are fixed at their starting values, as are the orientations and positions of the two formamide fragments relative to the peptide backbone, each defined by one distance, two angular, and three dihedral angle restraints.

Table S1. Experimental N-H RDCs of 5 GB3 mutants. The RDCs of each mutant are scaled to produce $Da \approx 10\text{Hz}$.

Residue	K19AD47K	K19ED40N	K19EK4A-C- His ₆	K19EK4A-N- His ₆	K19AT11K
3	-8.831	13.148	-9.503	-11.378	-15.477
4	-5.908	20.057	-13.106	-13.075	-11.522
5	-6.669	9.532	-6.603	-10.257	-1.991
6	-5.216	10.068	-3.159	-11.028	-5.03
7	-4.337	-2.381	-0.795	-8.015	3.143
8	-7.248	-2.561	7.401	-7.313	-4.12
9	-1.403	-2.413	-2.651	-3.136	7.761
10	-9.646	-10.478	N/A	-6.318	-7.318
11	-8.625	-6.683	N/A	-0.271	-5.03
12	-5.358	0.923	-3.862	-8.985	-3.044
13	-4.913	12.244	-6.041	-10.286	-5.647
14	-6.545	10.961	-6.555	-11.185	-4.716
15	-6.345	10.548	-6.745	-11.554	-5.517
16	-5.823	14.795	-8.994	-11.292	-6.3
17	-6.724	17.333	-11.34	-12.768	-11.851
18	-4.235	16.124	-13.706	-12.266	-14.836
19	-4.478	13.842	-13.048	-11.98	-14.697
20	-2.9	0.178	-5.959	-9.232	-12.158
21	-4.855	2.851	-6.923	-10.013	-14.182
22	8.617	13.704	-13.392	-5.178	-6.871
23	6.814	16.257	-14.06	-6.823	-8.573
24	13.435	N/A	N/A	7.108	4.377
25	N/A	N/A	N/A	4.907	5.073
26	9.603	15.263	-15.032	-4.2	-6.094
27	9.37	13.286	-7.956	-0.651	-3.115
28	15.819	3.482	-1.686	11.53	8.961
29	15.378	8.355	-13.037	1.938	0.777

30	9.648	14.394	-10.87	-1.682	-3.575
31	9.586	5.115	2.483	8.284	3.624
32	18.319	-0.07	-3.781	13.767	11.808
33	14.912	9.236	-10.44	4.043	1.876
34	9.134	11.821	-5.181	1.316	-1.538
35	N/A	2.399	2.709	11.956	7.068
36	18.136	2.848	-6.529	10.548	8.546
37	5.624	16.841	-11.467	-5.218	-6.566
38	-7.518	-8.426	20.017	6.5	-2.252
39	2.764	-7.341	12.059	16.999	12.422
40	-0.343	-6.811	17.124	11.303	3.564
41	-0.099	-8.135	16.849	11.117	6.394
42	-8.711	-9.641	18.406	1.09	-4.237
43	-5.528	-9.203	3.766	-8.621	-0.613
44	-6.061	9.363	-4.326	-11.103	-3.498
45	-7.255	11.144	-6.366	-10.579	-3.625
46	-7.175	17.121	-10.876	-12.274	-8.454
47	-4.162	3.553	-5.598	-4.789	3.294
48	4.532	-3.774	1.928	11.868	14.888
49	9.268	-9.579	-3.297	7.619	16.901
50	-5.21	16.556	-9.528	-11.525	-7.224
51	-7.808	18.331	-12.075	-12.818	-12.644
52	-7.321	11.522	-7.132	-8.33	-2.486
53	-6.054	6.176	-2.486	-10.961	-3.698
54	-5.946	-0.957	-0.603	-9.455	-0.143
55	-6.058	1.31	4.217	-8.846	-4.087
56	-5.579	-7.386	2.308	-8.397	0.874

Table S2. Experimental C'-H^N RDCs of 5 GB3 mutants. The C'-H^N RDCs of each mutant are scaled by the same factor as corresponding N-H RDCs.

Residue	K19AD47K	K19ED40N	K19EK4A- C-His ₆	K19EK4A- N-His ₆	K19AT11K
3	2.363	2.129	-5.093	-2.755	-3.044
4	-3.706	2.665	-0.433	-0.671	-1.458
5	0.008	6.239	-2.966	-3.313	-3.502
6	-2.401	3.359	-2.172	-1.749	-0.194
7	-1.277	4.14	-1.13	-3.259	-2.404
8	-1.601	0.845	-1.801	-2.781	0.914
9	-2.449	4.984	N/A	-3.442	-2.427
10*	1.631	-3.374	N/A	-1.335	0.552
11*	-4.379	-2.668	N/A	1.31	-2.035
12*	-1.503	1.644	0.442	-1.883	-2.602
13	-1.294	-1.639	0.063	-2.489	0.958
14	0.351	N/A	N/A	-1.773	-2.183
15	-0.587	-0.393	-0.091	0.823	N/A

16	-0.844	2.544	0.405	-1.971	-1.773
17	-3.052	1.316	1.157	0.56	0.047
18	1.49	5.524	-3.203	-2.114	-2.579
19	-4.853	1.001	1.698	-0.515	-3.069
20	0.099	5.815	-5.212	-3.584	-4.61
21	-5.136	-3.774	4.922	-2.54	N/A
22*	6.519	-0.762	-2.409	4.243	4.282
23	-3.08	6.403	-3.916	-4.649	-4.792
24*	-0.774	N/A	N/A	0.989	-0.555
25*	N/A	N/A	N/A	5.204	7.081
26	0.156	1.664	-3.778	-3.217	-4.643
27	-1.491	5.161	-2.484	-4	-2.778
28	0.275	-1.913	5.362	4.715	2.249
29	5.567	-2.601	-3.057	2.286	4.433
30	-1.106	5.98	-4.809	-4.017	-5.39
31	-1.738	0.429	2.92	-1.142	-1.602
32	2.955	-2.569	3.07	6.425	6.183
33	4.359	-0.475	-4.571	-0.098	0.663
34	-1.059	6.792	-4.286	-4.25	-4.009
35*	N/A	-1.973	5.485	1.772	-0.633
36	5.377	-2.743	-0.546	5.257	7.379
37	-1.063	5.128	-4.668	-3.594	-5.592
38	-3.381	-3.12	4.24	-1.948	-1.886
39	5.733	-0.74	0.114	5.239	4.889
40*	-0.209	-2.243	3.726	4.338	3.257
41*	2.996	-0.448	1.42	2.045	2.1
42	-4.543	-2.146	2.848	-1.56	-4.653
43	-2.323	-1.097	4.579	-0.696	-1.603
44	-0.47	-2.927	-0.336	-1.997	2.293
45	0.223	6.462	-3.09	-3.358	-3.69
46	-1.365	-0.043	-1.438	-2.081	1.864
47	-1.91	4.582	N/A	-4.223	-2.511
48	-3.612	-0.243	3.325	1.617	-0.534
49	6.562	-1.406	-2.57	3.868	5.013
50	-2.386	0.241	0.947	-3.408	-1.141
51	-2.791	1.314	0.695	1.18	0.746
52	-2.047	6.429	-4.675	-4.139	-5.58
53	-0.625	0.002	-1.169	-0.533	3.315
54	-0.695	4.98	-2.478	-3.1	-3.016
55	-1.016	0.475	-1.383	-2.122	2.306
56	-1.487	2.285	1.188	-2.217	-1.883

* Residues not included in the uniform bond length fitting.

Table S3. Experimental N-H RDCs of 6 GB3 mutants. The RDCs of each mutant are scaled to produce $Da \approx 10\text{Hz}$. The N-H RDCs were obtained from different measurements in different time (see supplementary text). As a result, the N-H RDCs are slightly different from those in Table S1.

Residue	K19AD47 K	K19ED40 N	K19EK4 A-C-His ₆	K19EK4 A-N-His ₆	K19AT11 K	K19EK4 A
3	-9.011	14.211	-8.884	-11.599	-15.448	-10.559
4	-5.982	19.744	-12.991	-13.076	-11.783	-14.568
5	-7.161	9.511	-6.312	-10.149	-1.993	-7.224
6	-5.59	10.088	-3.089	-11.398	-4.981	-7.409
7	-4.718	-2.286	-0.711	-8.019	3.054	-1.801
8	-7.293	-2.589	7.778	-7.337	-4.067	5.642
9	-1.895	-2.266	-2.771	-3.193	7.882	-3.727
10	-9.777	-10.394	N/A	-6.329	-7.413	8.931
11	-8.381	-6.56	N/A	-0.328	-5.044	13.614
12	-5.41	0.94	-3.716	-9.201	-3.013	-3.397
13	-5.196	12.554	-5.935	-10.748	-5.691	-8.38
14	-6.985	10.953	-6.523	-11.231	-5.012	-8.099
15	-6.75	10.855	-6.68	-11.401	-5.33	-7.803
16	-6.336	14.767	-8.855	-11.457	-6.387	-12.099
17	-7.148	17.16	-11.549	-12.743	-11.723	-13.087
18	-4.337	15.818	-13.548	-11.961	-14.762	-14.999
19	-4.763	13.363	-12.898	-12.13	-14.754	-14.019
20	-2.709	0.298	-5.669	-9.046	-12.106	-5.768
21	-4.511	2.848	-6.252	-9.818	-14.194	-7.215
22	8.771	13.419	-13.701	-4.729	-6.836	-16.901
23	6.76	16.224	-14.028	-6.895	-8.78	-16.582
24	13.22	7.386	-4.182	7.033	4.521	-4.484
25	17.188	4.274	-12.422	5.149	4.946	-12.033
26	9.678	14.902	-14.866	-4.392	-6.011	-16.633
27	9.494	13.593	-7.63	-0.706	-3.448	-10.21
28	15.523	3.449	-2.117	11.898	8.916	-1.484
29	15.335	8.366	-13.157	1.978	0.834	-13.526
30	9.791	14.342	-11.068	-1.571	-3.741	-13.589
31	9.532	6.202	2.563	8.443	3.655	1.306
32	18.043	0.253	-4.084	13.345	11.784	-2.792
33	15.183	9.178	-10.561	4.012	1.894	-11.467
34	9.241	11.464	-4.811	1.481	-1.456	-7.688
35	11.693	2.38	2.681	12.107	7.394	2.346
36	17.709	3.266	-6.902	10.303	8.519	-5.982
37	5.419	17.229	-11.316	-5.153	-6.612	-15.426
38	-7.15	-7.974	20.036	6.905	-2.138	19.634
39	2.914	-7.509	11.718	17.119	12.4	14.589
40	-0.148	-6.576	17.037	11.053	3.719	16.97
41	0.072	-8.262	16.603	11.184	6.286	14.692

42	-8.76	-9.69	18.623	0.914	-4.278	17.026
43	-5.833	-9.595	4.046	-8.462	-0.386	3.428
44	-6.219	9.342	-4.005	-11.118	-3.298	-5.985
45	-7.753	10.772	-6.25	-10.345	-3.462	-8.465
46	-7.38	17.181	-10.073	-11.829	-8.391	-10.955
47	-4.749	4.464	-4.648	-4.968	3.488	-4.631
48	4.315	-3.516	1.575	11.765	14.876	4.728
49	8.819	-9.553	-3.732	7.614	16.779	-0.424
50	-5.69	16.711	-9.272	-11.793	-7.419	-12.748
51	-8.282	18.282	-11.398	-12.46	-12.525	-13.101
52	-7.947	11.116	-6.996	-8.333	-2.311	-8.398
53	-6.334	6.523	-2.268	-11.227	-3.742	-3.693
54	-6.265	-0.58	-0.289	-9.534	0.16	-0.167
55	-6.318	1.94	4.388	-9.052	-4.296	2.219
56	-5.6	-7.666	2.555	-8.417	0.863	2.065

- (1) Tolman, J. R. *J. Am. Chem. Soc.* **2002**, *124*, 12020-12030.
- (2) Yao, L.; Vogeli, B.; Torchia, D. A.; Bax, A. *Journal of Physical Chemistry B* **2008**, *112*, 6045-6056.
- (3) Lienin, S. F.; Breimi, T.; Brutscher, B.; Bruschweiler, R.; Ernst, R. R. *J. Am. Chem. Soc.* **1998**, *120*, 9870-9879.
- (4) Bouvignies, G.; Bernado, P.; Meier, S.; Cho, K.; Grzesiek, S.; Bruschweiler, R.; Blackledge, M. *Proc. Natl. Acad. Sci. U. S. A.* **2005**, *102*, 13885-13890.
- (5) McGervey, J. D. *Quantum Mechanics Concepts and Applications*; Academic Press: New York, 1995.
- (6) McQuarrie, D. A. *Statistical Mechanics*; Harper and Row: New York, 1976.
- (7) Henry, E. R.; Szabo, A. *J. Chem. Phys.* **1985**, *82*, 4753-4761.
- (8) Case, D. A. *J. Biomol. NMR* **1999**, *15*, 95-102.
- (9) Mayer, J. E.; Mayer, M. G. *Statistical Mechanics*; Wiley: New York, 1940.
- (10) Cornilescu, G.; Bax, A. *J. Am. Chem. Soc.* **2000**, *122*, 10143-10154.
- (11) Vogeli, B.; Yao, L. S.; Bax, A. *J. Biomol. NMR* **2008**, *41*, 17-28.
- (12) Hall, J. B.; Fushman, D. *J. Biomol. NMR* **2003**, *27*, 261-275.
- (13) Gaussian 03, Revision **C.02**, Frisch, M. J.; Trucks, G. W.; Schlegel, H. B.; Scuseria, G. E.; Robb, M. A.; Cheeseman, J. R.; Montgomery, Jr., J. A.; Vreven, T.; Kudin, K. N.; Burant, J. C.; Millam, J. M.; Iyengar, S. S.; Tomasi, J.; Barone, V.; Mennucci, B.; Cossi, M.; Scalmani, G.; Rega, N.; Petersson, G. A.; Nakatsuji, H.; Hada, M.; Ehara, M.; Toyota, K.; Fukuda, R.; Hasegawa, J.; Ishida, M.; Nakajima, T.; Honda, Y.; Kitao, O.; Nakai, H.; Klene, M.; Li, X.; Knox, J. E.; Hratchian, H. P.; Cross, J. B.; Bakken, V.; Adamo, C.; Jaramillo, J.; Gomperts, R.; Stratmann, R. E.; Yazyev, O.; Austin, A. J.; Cammi, R.; Pomelli, C.; Ochterski, J. W.; Ayala, P. Y.; Morokuma, K.; Voth, G. A.; Salvador, P.; Dannenberg, J. J.; Zakrzewski, V. G.; Dapprich, S.; Daniels, A. D.; Strain, M. C.; Farkas, O.; Malick, D. K.; Rabuck, A. D.; Raghavachari, K.; Foresman, J. B.; Ortiz, J. V.; Cui, Q.; Baboul, A. G.; Clifford,

S.; Cioslowski, J.; Stefanov, B. B.; Liu, G.; Liashenko, A.; Piskorz, P.; Komaromi, I.; Martin, R. L.; Fox, D. J.; Keith, T.; Al-Laham, M. A.; Peng, C. Y.; Nanayakkara, A.; Challacombe, M.; Gill, P. M. W.; Johnson, B.; Chen, W.; Wong, M. W.; Gonzalez, C.; and Pople, J. A.; Gaussian, Inc., Wallingford CT, 2004.